J Fluoresc (2008) 18:685–693
DOI 10.1007/s10895-008-0344-z

ORIGINAL PAPER

Preparation, Characterization and Photophysical Properties of Highly Luminescent Terbium Complexes Incorporated Into SiO_2/Polymer Hybrid Material

Li Xu · Yu-Fei Ma · Kuan-Zhen Tang · Yu Tang · Wei-Sheng Liu · Min-Yu Tan

Received: 8 October 2007 / Accepted: 30 January 2008 / Published online: 15 February 2008

Abstract Two new highly luminescent Tb(III) coordination complexes of β-diketone ligands, $[TbL^{I}(NO_3)_3(H_2O)]$ 1 [L^{I}=*N*-(2-pyridinyl)ketoacetamide] and $[TbL^{II}{}_2(NO_3)_2(C_3H_6O)][TbL^{II}(NO_3)_4]$ 2 [L^{II}=*N*-(6-(4-methylpyridinyl)) ketoacetamide], were synthesized and characterized by single crystal X-ray diffraction, and incorporated into SiO_2/polymer hybrid material by sol–gel method resulting in a novel ternary molecular hybrid material. The Tb(III) complexes display characteristic metal-centered luminescence while the ligands emission are completely quenched, showing that efficient ligand-to-metal energy transfer (antenna effect) occurs. The gels can exhibit the characteristic emission bands of terbium ion. In addition, terbium ions present longer fluorescence lifetime in gels than in the corresponding pure complexes powders. Compared with the complexes, the unit mass luminescence intensities of the gels are enhanced. And the increase extent of luminescence intensity of the gel is influenced by the substituent of the ligands. At the same time, concentration effects on the luminescence intensity were investigated. The photo stabilities of the gels under UV radiation are much better than those of the pure terbium complexes.

L. Xu · Y.-F. Ma · K.-Z. Tang · Y. Tang (✉) · W.-S. Liu · M.-Y. Tan
College of Chemistry and Chemical Engineering,
State Key Laboratory of Applied Organic Chemistry,
Lanzhou University,
Lanzhou 730000, People's Republic of China
e-mail: tangyu@lzu.edu.cn

Keywords Terbium complexes · β-Diketone ligands · Hybrid materials · SiO_2/polymer matrix · Photophysical properties

Introduction

The trivalent lanthanide ions are well-known for their photoluminescence properties in the visible and near-infrared regions. Due to the poor absorption abilities of the lanthanide ions, it is common practice to form complexes of the lanthanide ions with organic ligands that can absorb light strongly and transfer the energy to the metal center (antenna effect) [1–9]. Since that time a lot of attention has been paid to the luminescence of molecular lanthanide compounds, and especially to the β-diketonate complexes. In particular, some complexes in this category have been noted to show laser action in solutions [10–12], therefore, they are expected to be promising luminescent dopants for the preparation of hybrid phosphors and other optical sources. The organic β-diketone ligands play an important role in the high optical function of the complexes because they have a high coefficient of absorption. High energy transfer efficiency can be achieved when appropriate organic β-diketone are selected [13, 14]. It has been reported that ligand-to-metal energy transfer of europium and terbium β-diketonate chelates is affected significantly on changing substituents in the organic ligand. An increase in the conjugation by attaching aromatic substituents, such as *p*-phenyldibenzoyl methide, dinaphthoyl methides, to β-diketonate can result in enhanced metallic emission [15]. *N*-(2-Pyridinyl)ketoacetamide and *N*-(6-(4-methylpyridinyl))ketoacetamide are potential ligands

with simple and flexible structure and perfect yield to synthesize. So the lanthanide complexes with these β-diketonate ligands are expected to be promising luminescent dopants with intense emission and cheap cost.

Although lanthanide complexes exhibit a much more efficient emission under ultraviolet excitation [16], up to the present day they have been excluded from practical applications as tunable solid-state lasers or phosphor devices due to their poor thermal stability and mechanical properties [17]. In order to circumvent these shortcomings, the lanthanide complexes can be incorporated into inorganic and/or inorganic–organic matrices using low-temperature soft-chemistry processes, such as the sol–gel route. The sol–gel process is a promising technique for the development of novel luminescent materials due to its mild reaction conditions, versatility of processing and potential for mixing the inorganic and organic precursor components at the nanometer scale [18, 19]. When functional active molecules, such as optical, electronic, magnetic and biological species, are incorporated into the hybrid structure, functional organic–inorganic hybrid nanocomposites may be thus synthesized. Indeed, much work has been focused on this field to date, and many lanthanide complexes have been incorporated into sol–gel derived matrices or other solid hosts such as zeolite, layered or mesoporous matrices [20–28]. However, much of these works have focused on doping with lanthanide complexes of conventional β-diketone ligands such as 2-thenoyltrifluoroacetonate [29, 30], and focused on the comparison of the luminescent properties between the silica gels doped with lanthanide complexes and the corresponding chlorides, and little attention has been paid to the changes of luminescence properties of lanthanide complexes in silica gels compared with the original complexes. Additionally, conventional gels tend to crack during the drying period owing to their poor mechanical strength and the SiO_2 matrix containing –OH can extensively reduce luminescence emission intensity and decay time. One strategy is to introduce polymer into inorganic matrix. Such inorganic/polymer hybrid matrixes allow for increasing solubility of complexes in the sol-gel matrix while variation of the percentage of the inorganic/polymer components allows for modification of both mechanical and optical properties of the materials [31–34]. Polyvinyl butyral (PVB) is a polymer with good thermal stability. Therefore, in this work, we will introduce two new highly luminescent Tb(III) complexes of β-diketone ligands, $[TbL^{I}(NO_3)_3(H_2O)]$ 1 [L^{I}=*N*-(2-pyridinyl)ketoacetamide] and $[TbL^{II}{}_2(NO_3)_2(C_3H_6O)]$ $[TbL^{II}(NO_3)_4]$ 2 [L^{II}=*N*-(6-(4-methylpyridinyl))ketoacetamide], into a sol–gel derived SiO_2/PVB matrix which is a kind of non-crystalline substance with porous structure, and systematically investigate the luminescent properties, concentration effects on luminescence intensity, luminescence lifetime and the photo-stabilities under UV radiation with respect to the corresponding pure complexes.

Experimental section

Synthesis of the ligands L^{I} and L^{II}

The ligand L^{I} was prepared by the reaction of 2-aminopyridine with ethyl acetoacetate, as described previously [35], yield 80%, m.p. 109 °C–110 °C. Anal. Calcd. for $C_9H_{10}N_2O_2$: C, 60.67; H, 5.61; N, 15.73; Found: C, 60.58; H, 5.62; N, 15.71%; ^{1}H NMR ($CDCl_3$, 300 MHz): 1.99 (s, 3H), 3.63 (s, 2H), 5.06 (s, 1H), 6.99–7.28 (1H),7.61–7.82, 8.12–8.36 (2H), 9.56 (s, 1H), 13.48 (s, 1H); IR (KBr pellet, cm^{-1}): ν(C=O) 1,723 (s), 1,668 (s); ν(N–H) 3,254 (m), 3,100 (m), 3,036 (m) and ν(O–H) 3,200 (m).

The ligand L^{II} was prepared by the reaction of 2-amino-4-picoline with ethyl acetoacetate, as described previously [35], yield 75%, m.p. 108 °C–110 °C. Anal. Calcd. for $C_{10}H_{12}N_2O_2$: C, 62.49; H, 6.29; N, 14.57; Found: C, 62.50; H, 6.30; N, 14.55%; ^{1}H NMR ($CDCl_3$, 300 MHz): 1.99 (s, 3H), 2.34 (s, 3H), 3.60 (s, 2H), 4.97 (s, 1H), 6.67–6.96 (1H), 7.28–8.01 (2H), 9.06 (s, 1H), 13.46 (s, 1H); IR (KBr pellet, cm^{-1}): ν(C=O) 1723 (s), 1,668 (s); ν(N–H) 3260 (m), 3,100 (m), 3,040 (m) and ν(O–H) 3,215 (m).

Synthesis of the terbium complexes

The solution of 0.3 mmol ligand (L^{I} or L^{II}) in chloroform (2 cm^3) was added dropwise to a solution of 0.1 mmol Tb $(NO_3)_3{\cdot}6H_2O$ in ethyl acetate (2 cm^3). Then the mixture was stirred at room temperature for 4 h. And the precipitated solid complex was filtered, washed with mixed solvent of chloroform and ethyl acetate (V/V=1:1), dried in vacuo over P_4O_{10} for 48 h. Single crystals of the terbium complexes were grown from acetone and chloroform mixed solutions with slow evaporation at room temperature. After approximately 1 month, transparent colorless crystals were formed from the solutions respectively.

Preparation of SiO_2/PVB hybrid material doped with the terbium complexes

In a typical run, TEOS was first mixed with absolute ethanol. Then HCl-acidified water (pH=2) was added to the above mixture under magnetic stirring to initial the hydrolysis and condensation reaction. The molar ratio of TEOS/ethanol/H_2O is 1:4:4. A transparent sol was obtained. After stirred for several hours, absolute ethanol solutions containing different contents of terbium complexes and PVB were added to the sol. The content of PVB is 10% by weight referring to the SiO_2 content. The sols

were poured into plastic boxes with sealed caps. The transparent monolithic gels were allowed to age for several days before heat-treating at 80 °C for 1 day.

Materials and physical measurements

Terbium nitrate was prepared according to the literature methods [36]. All the solvents and reagents for synthesis including tetraethoxysilane (TEOS, Acros Chemical Co.) were commercially available, analytical grade, and used as received. All characterizations were carried out using a fresh sample. Elemental analyses were determined on an Elementar Vario EL analyzer. IR spectra were recorded on a Nicolet 360 FT-IR instrument using KBr discs in the 4,000–400 cm^{-1} region. ^1H NMR spectra were measured on a Varian Mercury 300 spectrometer in $CDCl_3$ solutions. The UV-visible spectra were measured using a Lambda 35 spectrometer. Luminescence and phosphorescence spectra were obtained on a Hitachi F-4500 spectrophotometer. The fluorescence lifetime measurements were performed on an Edinburgh FLS920 time-resolved fluorescence spectrophotometer. For photo stability experiments, the samples were irradiated using a 30-W high-pressure mercury lamp, the distance between the samples and the center of the lamp was 10 cm.

Single crystal X-ray diffraction data were recorded on a Bruker Smart-APEX diffractometer equipped with a CCD detector with Mo Kα radiation (λ=0.71073 Å). The unit cell parameters and integrations of the diffraction profiles were determined using SAINT program [37]. Structure solution and full-matrix least-squares refinement based on F^2 were performed with the Shelxs-97 and Shelxl-97 program packages [38], respectively. Terbium centers were located from the *E*-map and other non-hydrogen atoms were located in successive difference Fourier syntheses. The final refinements were performed by full matrix least-squares methods with anisotropic thermal parameters for non-hydrogen atoms on F^2. All the hydrogen atoms were first found in difference electron density maps, and then placed in the calculated sites and included in the final refinement in the riding model approximation with displacement parameters derived from the parent atoms to which they were bonded. Final $R = \sum(||F_o| - |F_c||)/\sum|F_o|$, and $wR = \left[\sum w\left(F_o^2 - F_c^2\right)^2 \Big/ \sum w\left(F_o^2\right)^2\right]^{1/2}$, with $w = 1\Big/[\sigma^2\left(F_o^2\right) + (aP)^2 + bP]$ (where $P = \left(\max\left(F_o^2, 0\right) + 2F_c^2\right)/3$). Details on crystal data and intensity data were given in Table 1.

Table 1 Crystallographic data and structure refinement summary for complex 1 and complex 2

	1	2
Chemical formula	$C_9H_{10}N_5O_{12}Tb$	$C_{33}H_{42}N_{12}O_{25}Tb_2$
Formula weight	539.14	1324.63
Temperature (K)	294(2)	298(2)
Wavelength (Å)	0.71073	0.71073
Crystal system	Triclinic	Triclinic
Space group	$P\bar{1}$	$P\bar{1}$
A (Å)	7.4649(3)	9.109(2)
B (Å)	10.6199(5)	12.544(3)
C (Å)	11.7150(5)	22.250(5)
α (°)	68.418(2)	98.462(3)
β (°)	87.426(2)	97.266(2)
γ (°)	86.611(2)	104.104(2)
V (Å^3), *Z*	861.83(6), 2	2403.7(9), 2
Calculated density (g cm^{-3})	2.078	1.830
Absorption coefficient (mm^{-1})	4.177	3.016
F(000)	520	1308
Crystal size (mm)	0.37×0.27×0.26	0.29×0.25×0.20
θ range for data collection (°)	1.87, 25.50	2.29, 25.76
Limiting indices	−9<h<8; −12<*k*<12; −9<l<14	−10<*h*<10; −14<*k*<14; −26<l<26
Reflections collected/ unique	4,566/3,125 [*R*(int)= 0.0119]	12,617/8,346 [*R* (int)=0.0232]
Completeness to θ	θ=25.50, 97.4%	θ=25.01, 98.6%
Refinement method	Full matrix least-squares	Full matrix least-squares
Data/restraints/ parameters	3,125/162/246	8,346/144/649
Goodness-of-fit on F^2	1.060	1.043
Final *R* indices	*R*=0.0230, w*R*=0.0538	*R*=0.0405, w*R*= 0.0849
R (all data)	*R*=0.0251, w*R*=0.0550	*R*=0.0644, w*R*= 0.0948
Largest diff peak and hole (e/nm^3)	967 and −700	802 and −689

Results and discussion

The crystal structures of the complexes 1 and 2 with the numbering scheme are displayed in Fig. 1a and b. Important experimental parameters of the single-crystal X-ray analysis of the complex 1 reveals that isolated mononuclear Tb atom is coordinated with nine oxygen donor atoms. Six of them belong to three bidentate nitrate groups, two belong to *O*, *O*-bidentate L^I and one belong to water molecule. The coordination polyhedron around Tb^{3+} is a distorted tricap-

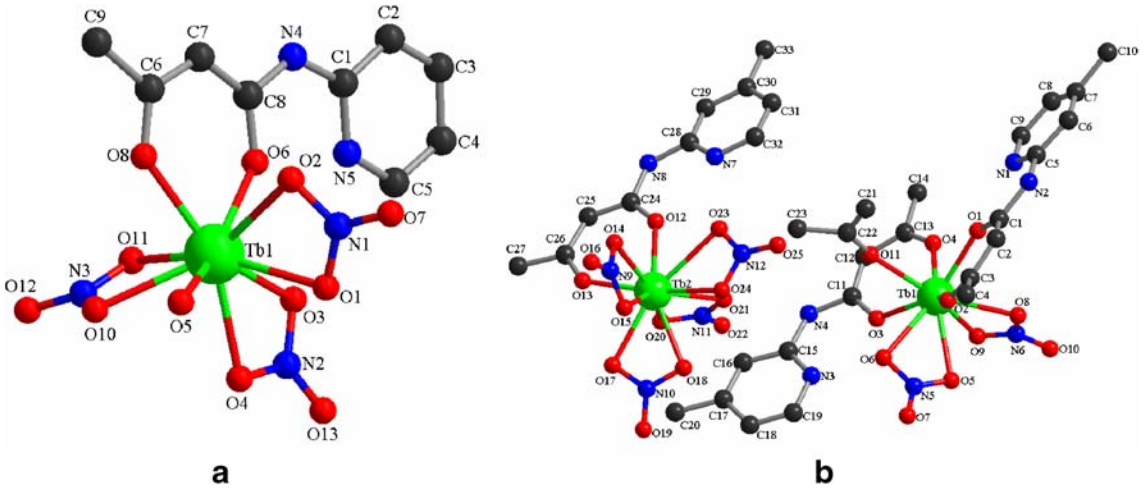

Fig. 1 X-Ray structure of the terbium complex 1 (**a**) complex 2 (**b**)

ped trigonal prism. β-Diketones coordinated to metal ions usually exist as the enol tautomer with a negative charge (dehydrogen form). From the C–O distances and it's connected C–C bond distances we can determine the main structure of the β-diketone bonded to the lanthanide ions [39]. In the structure of complex 1, the average distances for the carbon-carbon bonds (C(6)–C(7), 1.390(5) Å; C(7)–C(8), 1.400(5) Å) and the carbon–oxygen bonds (C(6)–O(8), 1.288(4) Å; C(8)–O(6), 1.263(4) Å) are between the single bond distance and double bond distance. This can be explained by the fact that there exists conjugated structure between the enol bond and the coordinated β-diketonate, which lead to the delocalization of electron density of the coordinated β-diketonate chelate ring. The enol hydrogen atom H(4A) bonded to the carbonyl oxygen atom was disengaged and bonded to the nitrogen atom from pyridyl ring, since the complex was stirred at the neutral condition. The Tb–O bond distances (2.315(3)–2.296(2) Å) are similar to those found for the lanthanide complexes of β-diketonate [40].

It can be seen from Fig. 1b that the complex 2 consists of a complex cation $[TbL^{II}_2(NO_3)_2(C_3H_6O)]^+$ and a complex anion $[TbL^{II}(NO_3)_4]^-$. In the $[TbL^{II}_2(NO_3)_2(C_3H_6O)]^+$ coordination cation, the Tb^{3+} ion is nine-coordinated and surrounded by two *O*,*O*-bidentate L^{II}, two bidentate nitrate ions, and one acetone molecule to assume a distorted tricapped trigonal prism geometry. The Tb–O bond distances [2.328(4)–2.357(4) Å], the carbon–carbon bond distances [C(13)–C(12), 1.393(9) Å; C(12)–C(11), 1.375 (8) Å] and the carbon–oxygen bonds[C(13)–O(4), 1.285 (8) Å; C(11)–O(3), 1.264(7) Å] are close to those observed in complex 1. In the anion of $[TbL^{II}(NO_3)_4]^-$, the Tb^{3+} is coordinated with ten oxygen donor atoms. Eight of them belong to four bidentate nitrate groups, and the other two are from *O*,*O*-bidentate L^{II}. The coordination polyhedron around Tb^{3+} is a distorted bicapped square antiprism. The

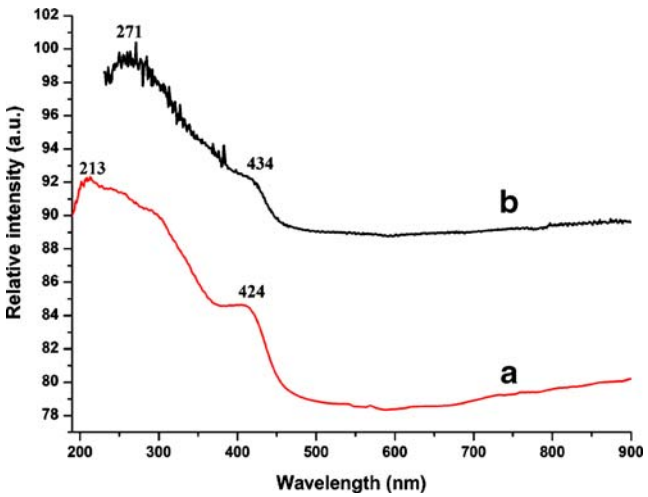

Fig. 2 UV-visible absorption spectra for SiO_2/PVB hybrid doped with complex 1 (**a**) and pure complex 1 (**b**)

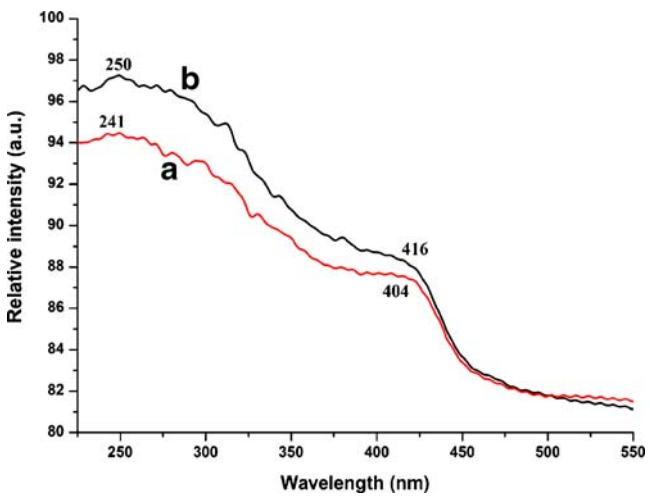

Fig. 3 UV-visible absorption spectra for SiO_2/PVB hybrid doped with complex 2 (**a**) and pure complex 2 (**b**)

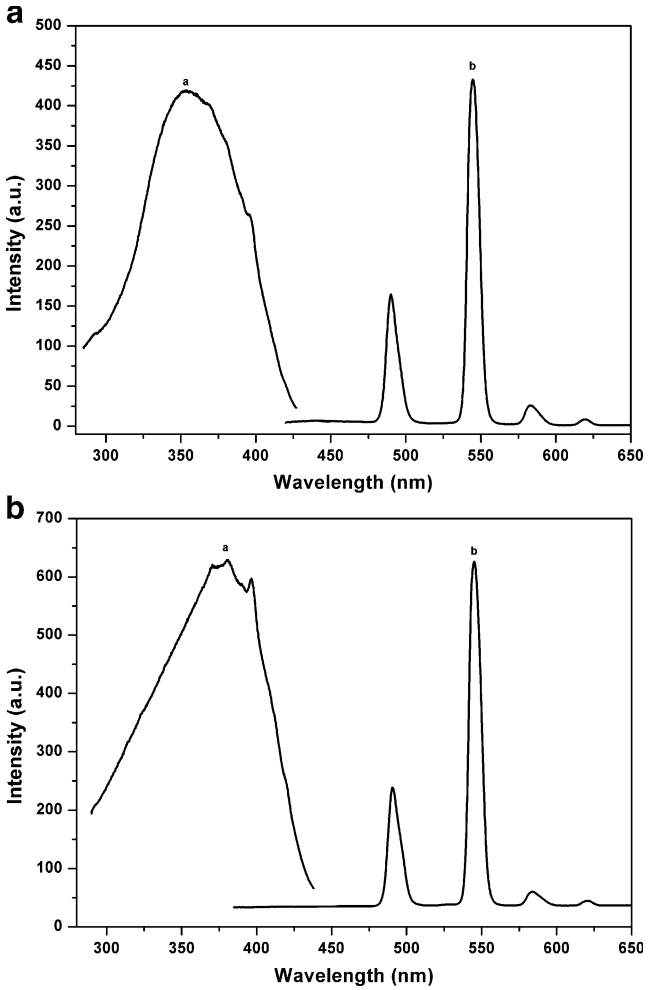

Fig. 4 Excitation spectra (**a**) and emission spectra (**b**) of SiO_2/PVB hybrid doped with complex 1 (**a**) and pure complex 1 powder (**b**)

Tb–O bond distances [2.308(5)–2.333(4) Å], the carbon–carbon bond distances [C(25)–C(26), 1.407(9) Å; C(24)–C(25), 1.372(9) Å] and the carbon–oxygen bonds [C(26)–O(13), 1.259(8); C(24)–O(12), 1.261(7) Å) are close to that observed in the complex cation.

The UV-visible absorption spectra of the SiO_2/PVB hybrid doped with complexes (complex 1, complex 2) and the pure terbium complexes (complex 1, complex 2) powders are shown in Figs. 2 and 3 respectively. It can be easily seen that the UV-visible spectrum of complex 1 has two main absorption peaks located at 271 and 434 nm (Fig. 2b), while the SiO_2/PVB hybrid doped with complex 1 gels also has two main absorption peaks at 213 and 424 nm (Fig. 2a). The spectrum of complex 2 has two main absorption peaks located at 250 and 416 nm (Fig. 3b). And for SiO_2/PVB hybrid doped with complex 2 gels, the main UV-visible absorptions are located at 241 and 404 nm (Fig. 3a). The UV-visible spectra can show the Tb complexes doped in the SiO_2/PVB hybrid. The micro-environments in the SiO_2/PVB hybrid result in blue shifts of the terbium complexes absorptions.

The excitation and emission spectra of SiO_2/PVB hybrid doped with the complex 1 (the content of the complex (wt%) is 7.8%) and pure complex 1 powder are shown in Fig. 4a and b, respectively. Both of the excitation spectra are broad bands and the emission spectra exhibit the characteristic emission of Tb^{3+} arising from the transition $^5D_4 \rightarrow {}^7F_J$ (J=6, 5, 4, 3), with the transition $^5D_4 \rightarrow {}^7F_5$ green emission as the dominant group. This strongly suggests that an efficient energy transfer form the ligands to Tb^{3+} can take place not only in the pure complex 1 but also in the SiO_2/PVB doped with complex 1.

Some differences in the excitation and emission spectra in Fig. 4a and b can be seen. For SiO_2/PVB hybrid doped with complex 1, the excitation spectrum consists of a relatively narrow band ranging from 295 to 425 nm with a maximum intensity at 354 nm, while the excitation spectrum changes into a broad band ranging from 285 to 430 nm with a maximum intensity at 371 nm for the pure

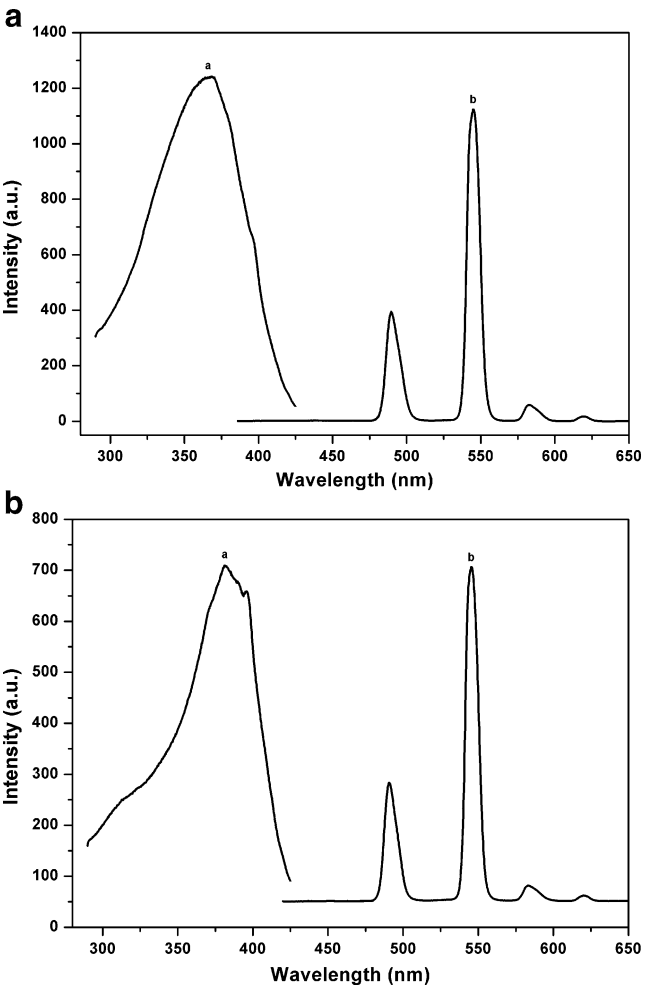

Fig. 5 Excitation spectra (**a**) and emission spectra (**b**) of SiO_2/PVB hybrid doped with complex 2 (**a**) and pure complex 2 powder (**b**)

Table 2 Relationship between the content of the Tb complex and luminescence intensity

Materials	Complex 1	SiO_2/PVB hybrid doped with complex 1	Complex 2	SiO_2/PVB hybrid doped with complex 2
The content of the complex (wt%)	100	7.8	100	7.8
Relative intensities of $^5D_4 \rightarrow {}^7F_5$	626	433	706	1,124

complex 1. Compared to the corresponding pure complex 1, the maximum excitation wavelength for the gel shows a blue shift, changing from 371 to 354 nm.

Figure 5 shows the excitation and emission spectra of SiO_2/PVB hybrid doped with the complex 2 (the content of the complex (wt%) is 7.8%; a) and pure complex 2 powder (b). Both of the emission spectra present the characteristic emission bands originating from the transition $^5D_4 \rightarrow {}^7F_J$ (J=6, 5, 4, 3), with the transition $^5D_4 \rightarrow {}^7F_5$ green emission as the dominant group. Compared to the pure complex 2, the maximum excitation wavelength of the gel shows a blue shift, changing from 396 to 368 nm.

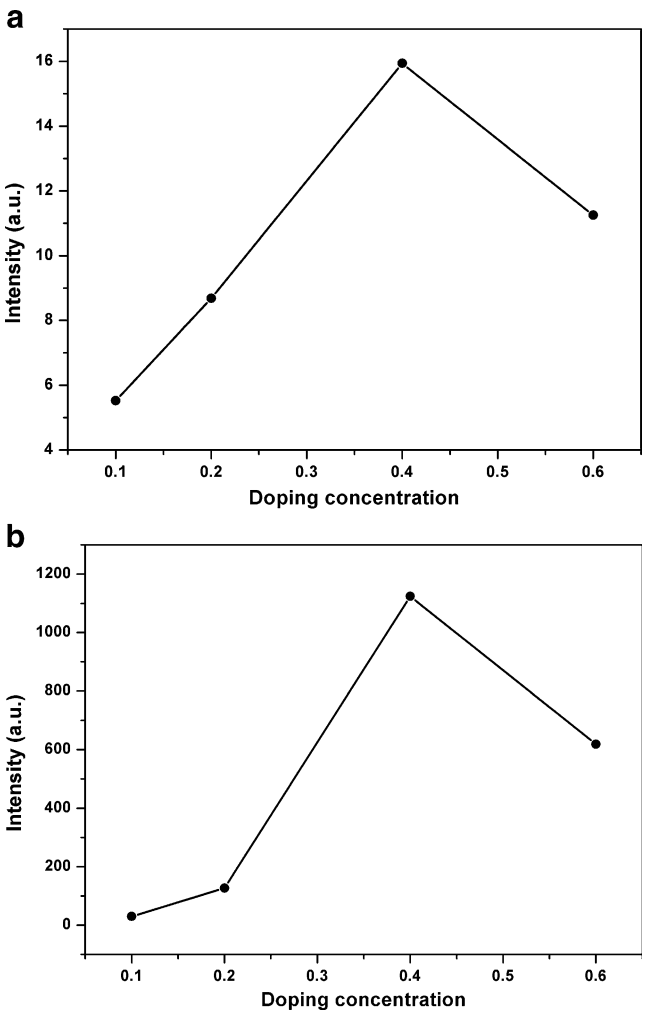

Fig. 6 The luminescence intensity distribution with the increment of the doping concentration of the complex 1 (**a**) and complex 2 (**b**)

The differences in the excitation spectra between SiO_2/PVB doped with the complexes and the pure complexes powders can be interpreted as follows. Compared to the pure complex, when the complex was doped into SiO_2/PVB, the polarity around the Tb^{3+} surrounding environment will increase, according to the Lippert equation [41], $hc\Delta\nu = 2\Delta f(\mu^* - \mu)^2/_{\alpha^3}$, where ν is the frequency shift (in cm^{-1}) of the excitation state, f is the orientation polarizability, μ^* and μ are the excited and ground state dipole moments, respectively, h is Planck's constant, c is the velocity of light and a is the cavity radius. Since the polarity of the complex in SiO_2/PVB is increased, Δf is a positive value. Therefore, $\Delta\nu$ is also a positive value. In other words, the excitation wavelengths of the gels show blue shifts compared to the pure complexes.

The content of the complexes in SiO_2/PVB hybrid matrix and its relative luminescence intensity compared with the complexes 1 and 2 ($^5D_4 \rightarrow {}^7F_5$) are listed in Table 2. It can be seen clearly that the complex of a unit mass in the SiO_2/PVB matrix can give stronger luminescence than the corresponding pure complex. Compared with the complexes 1 and 2, the luminescence intensity (the relative intensity divided by the mass) of the hybrid increases nine and twenty times respectively. As is known, the photophysical and photochemical process on guest molecule can be influenced profoundly by organized matrix. The SiO_2/PVB hybrid matrix, however, is a kind of non-crystalline substance with porous structure. This host can provide an interesting microchemical environment for the guest molecules. And we may deduce that when the complex is doped in the SiO_2/PVB matrix, the molecules were confined in micropores and the nonradiative transitions were decreased, resulting in high luminescence

Table 3 The fluorescence lifetimes of Tb ions in different materials

Materials	Lifetimes/μs
Complex 1	719
SiO_2/PVB hybrid doped with the complex 1	1,043
Complex 2	980
SiO_2/PVB hybrid doped with the complex 2	1,542

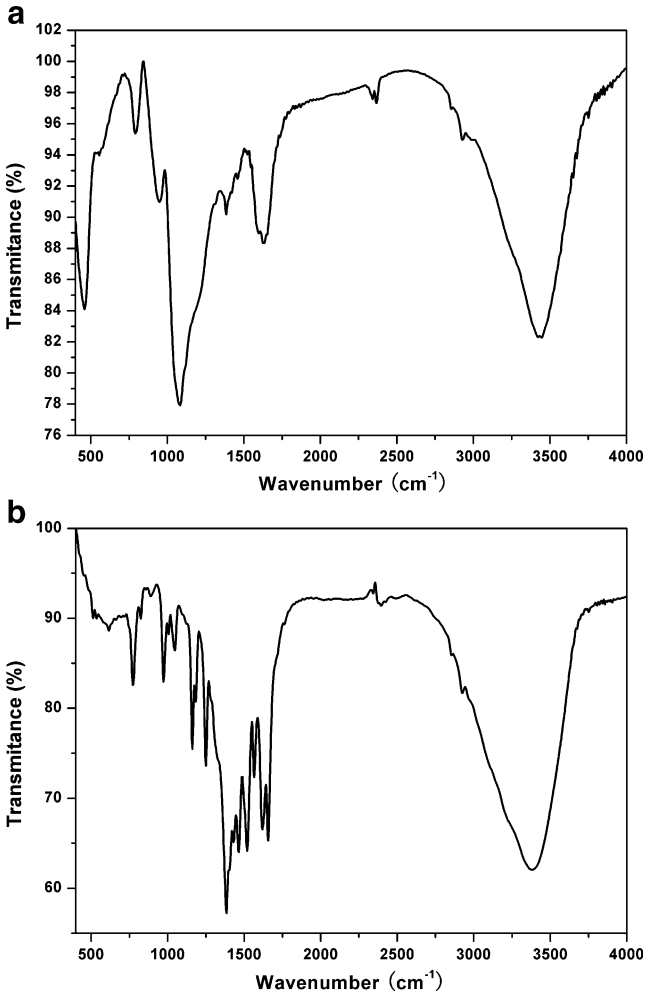

Fig. 7 Infrared spectra of SiO_2/PVB hybrid doped with complex 1 (**a**) and pure complex 1 powder (**b**)

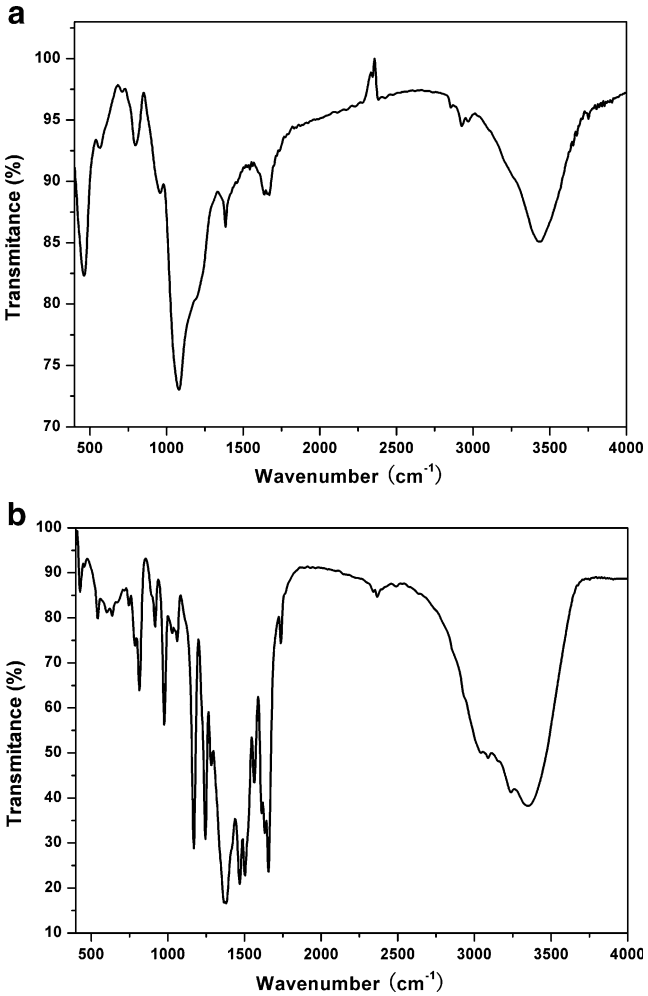

Fig. 8 Infrared spectra of SiO_2/PVB hybrid doped with complex 2 (**a**) and pure complex 2 powder (**b**)

efficiency. Moreover, the increase extent of luminescence intensity of the hybrid material doped with the complex 2 is obviously better than that doped with the complex 1. And we may infer that this result is caused by the difference between the substitutent of the ligands of these complexes.

In order to examine the doped concentration of complexes (complex 1 and complex 2) effect on the luminescence intensity, four different amounts, 0.1%, 0.2%, 0.4%, and 0.6% (molar ratio) of complexes (complex 1 and complex 2) were introduced into the SiO_2/PVB matrix. The relation curve diagrams between the intensity and doping concentrations were shown in Fig. 6a and b, respectively. As expected, the luminescence intensity increased with increasing the doped concentrations. However, the luminescence intensities for the gels doped with 0.6% of terbium complex show a decreasing value, indicating that optimal doped concentrations of these complexes are both 0.4% under the chosen experimental conditions.

The fluorescence decay curves of Tb^{3+} related to the transition $^5D_4 \rightarrow {}^7F_5$ emission in SiO_2/PVB matrix doped

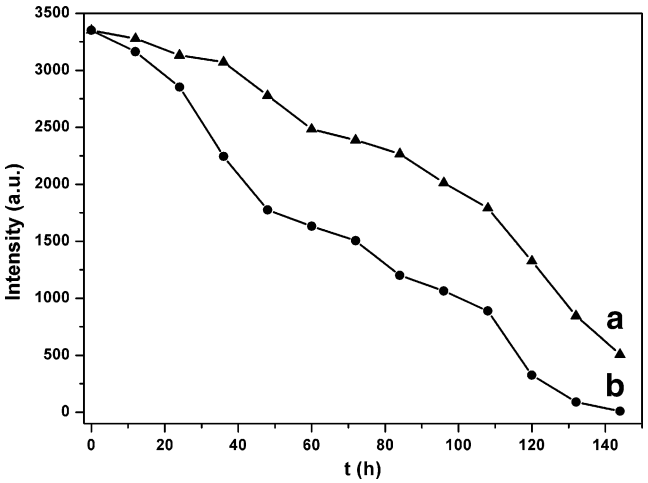

Fig. 9 Change of luminescence intensity of complex 1 in the SiO_2/PVB hybrid gels (**a**) and complex 1 (**b**) with the irradiation time

with complexes (complex 1, complex 2) and the pure terbium complexes (complex 1, complex 2) powders were measured and the lifetimes are summarized in Table 3.

It can be clearly seen that the terbium complexes doped into SiO_2/PVB have longer lifetimes than those of the corresponding pure complexes. It is well known that the fluorescence lifetime of Tb^{3+} is related to the vibration of the nearby ligands. The excitation energy of Tb^{3+} can be absorbed by the vibration of the ligands, thus, decreasing the lifetime of Tb^{3+}. The complete isolation of the complex molecules and the relatively rigid matrix structure has inhibited the vibration of the ligands around Tb^{3+}, leading to a longer fluorescence lifetime of Tb^{3+} in SiO_2/PVB matrix than those of in pure complex powder. This result is also supported by the IR spectra.

Figures 7 and 8 show the IR spectra of the SiO_2/PVB hybrid doped with complexes (complex 1, complex 2; Figs. 7a and 8a) and the pure terbium complexes (complex 1, complex 2) powders (Figs. 7b and 8b). In Figs. 7a and 8a, the broad band around 3,440 cm^{-1} is assigned to stretching vibrations of O–H groups, with 1,656 cm^{-1} corresponding to their bending vibration. The small peaks at around 2,960 cm^{-1} is assigned to asymmetric vibration of C–H band in $–CH_3$. And the band at 1,392 cm^{-1} is due to the symmetric stretching vibration of C–H. The high peaks at 1,083 and 800 cm^{-1} are attributed to Si–O–Si symmetric stretching vibration and bending vibration, respectively. The band at 457 cm^{-1} corresponds to the bending vibration of O–Si–O bond. The shoulder band at 962 cm^{-1} is related to the vibration of silanol groups. The characteristic absorption bands of the pure terbium complexes (complex 1, complex 2) powders (Figs. 7b and 8b) are not presented in Figs. 7a and 8a, reflecting that the vibrations of the ligands of Tb^{3+} have been confined by the surrounding rigid matrix. The restriction effect of the matrix on the vibrations of the molecules results in longer fluorescence lifetimes.

The photo stabilities of the complex 1 and the SiO_2/PVB hybrid gel were measured and the results are presented in Fig. 9. We employ the half-life $t_{1/2}$ to characterize the photo stability [42], where $t_{1/2}$ denotes the time taken for the fluorescent intensity to decrease to 50% of the initial value after irradiation under UV light. The $t_{1/2}$ values of complex 1 (Fig. 9b) and its SiO_2/PVB hybrid gel (Fig. 9a) are 60 and 108 h, respectively. It is easily found that the luminescent photo stability of the complex in the SiO_2/PVB hybrid gel is higher than that of the corresponding pure complex.

Conclusion

In this work, SiO_2/PVB hybrid materials doped with highly luminescent terbium complexes of β-diketone ligands have been prepared via a sol–gel method. For the hybrid materials, the energy transfer from the ligands to Tb ions took place smoothly, as for the original complexes, and consequently strong green emission based on Tb^{3+} were observed. The emission intensities of the gels doped with terbium complex increase with increasing the doping concentration within a certain range. Compared to the pure complexes, the excitation spectra of the SiO_2/PVB gel matrix doped with complexes show blue shifts. And the unit mass of the complexes in the SiO_2/PVB gel matrix can give stronger luminescence than the corresponding pure complexes. When the molecules were confined in micropores of the matrix and the nonradiative transitions were decreased, resulting in high luminescence efficiency. The increase extent of luminescence intensity of the hybrid material is influenced by the substitutent of the ligands of the complexes. The fluorescence lifetime of Tb^{3+} in the hybrid materials becomes longer than those in pure complexes. The photo-stabilities are improved after the complexes are doped into SiO_2/PVB gel matrix.

Acknowledgment The authors are grateful to the National Natural Science Foundation of China (project 20401008), the program for New Century Excellent Talents in University (NCET-06-0902) and the Natural Science Foundation of Gansu Province (project no. 3ZS061-A25-003). The cif files of the structures are available from the authors.

References

1. Weissman SI (1942) Intramolecular energy transfer the fluorescence of complexes of europium. J Chem Phys 10(4):214–217
2. Forsberg JH (1981) Gmelin handbook of inorganic chemistry, Sc, Y, La-Lu rare earth elements, 3rd edn. Springer, Berlin, pp 65–251 (and references therein)
3. Melby LR, Rose NJ, Abramson E, Caris JC (1964) Synthesis and fluorescence of some trivalent lanthanide complexes. J Am Chem Soc 86(23):5117–5125
4. Drake SR, Lyons A, Otway DJ, Slwain AMZ, Williams DJ (1993) Lanthanide b-diketonate glyme complexes exhibiting unusual coordination modes. J Chem Soc, Dalton Trans 15:2379–2386
5. Wang CY, Yang ZJ, Li Y, Gong LW, Zhao GW (2002) Preparation of thin films of ternary complex of europium with 2-thenoyltrifluoroacetone and *o*-phenanthroline. Phys Status Solid A 191 (1):117–124
6. Zhong GL, Kim K, Jin JI (2002) Intermolecular energy transfer in photo- and electroluminescence properties of a europium(III) complex dispersed in poly(vinylcarbazole). Synth Met 129 (2):193–198
7. Adachi C, Baldo MA, Forrest SR (2000) Electroluminescence mechanisms in organic light emitting devices employing a europium chelate doped in a wide energy gap bipolar conducting host. J Appl Phys 87(11):8049–8055
8. Sano T, Fujita M, Fujii T, Hamada Y, Shibata K, Kuroki K (1995) Novel europium complex for electroluminescent devices with sharp red emission. Jpn J Appl Phys 34(4A):1883–1887
9. Li HH, Inoue S, Machida K, Adachi G (1999) Preparation and luminescence properties of organically modified silicate composite phosphors doped with an europium(III) b-diketonate complex. Chem Mater 11(11):3171–3176

10. Samelson H, Lempicki A, Brophy VA, Brecher C (1964) Laser phenomena in europium chelates. I. Spectroscopic properties of europium benzoylacetonate. J Chem Phys 40(9):2547–2553
11. Bjorklund S, Kellermeyer G, Hurt CR, McAoy N, Filipescu N (1967) Laser action from terbium trifluoroacetylacetonate in *p*-dioxane and acetonitrile at room temperature. Appl Phys Lett 10 (5):160–162
12. Whittakker B (1970) Low threshold laser action of a rare earth chelate in liquid and solid host media. Nature 228:157–159
13. Dawson WR, Kropp JL, Windsor MW (1966) Internal-energy-transfer efficiencies in Eu^{3+} and Tb^{3+}chelates using excitation to selected ion levels. J Chem Phys 45(7):2410–2418
14. Crosby GA, Whan RE, Alire RM (1961) Intramolecular energy transfer in rare earth chelates. role of the triplet state. J Chem Phys 34(3):743–748
15. Filipescu N, Sager WF, Serafin FA (1964) Substituent effects on intramolecular energy transfer. II. Fluorescence spectra of eeuropium and terbium β-diketone chelates. J Phys Chem 68 (11):3324–3346
16. de Sá GF, Malta OL, de Mello Donegá C, Simas AM, Longo RL, Santa-Cruz PA, da Silva EF (2000) Spectroscopic properties and design of highly luminescent lanthanide coordination complexes. Coord Chem Rev 196(1):165–195
17. Dong DW, Jiang SC, Men YF, Ji XL, Jiang BZ (2000) Nanostructured hybrid organic–inorganic lanthanide complex films produced in situ via a sol-gel approach. Adv Mater 12(9):646–649
18. Binnemans K, Lenaerts P, Driesen K, Görller-Walrand C (2004) A luminescent tris(2-thenoyltrifluoroacetonato)europium(III) complex covalently linked to a 1,10-phenanthroline-functionalised sol–gel glass. J Mater Chem 14(2):191–195
19. Sanchez C, Lebeau B (2001) Design and properties of hybrid organic–inorganic nanocomposites for photonics. Mater Res Soc Bull 26:377–387
20. Matthews LR, Knobbe ET (1993) Luminescence behavior of europium complexes in sol–gel derived host materials. Chem Mater 5(12):1697–1700
21. Franville AC, Zambon D, Mahiou R, Troin Y (2000) Luminescence behavior of sol–gel-derived hybrid materials resulting from covalent grafting of a chromophore unit to different organically modified alkoxysilanes. Chem Mater 12(2):428–435
22. Bredol M, Jüstel T, Gutzov S (2001) Luminescence of sol–gel-derived silica doped with terbium-benzoate complex. Opt Mater 18(3):337–341
23. Qian GD, Wang MQ, Wang M, Fan XP, Hong ZL (1997) Synthesis in situ of 2,2¢-dipyridyl-Tb(III) complexes in silica gel. J Mater Sci Lett 16(4):322–323
24. Fu LS, Meng QG, Zhang HJ, Wang SB, Yang KY, Ni JZ (2000) In situ synthesis of terbium-benzoic acid complex in sol–gel derived silica by a two-step sol–gel method. J Phys Chem Solids 61 (11):1877–1881
25. Rosa ILV, Serra OA, Nassar EJ (1997) Luminescence study of the $[Eu(bpy)_2]^{3+}$ supported on Y zeolite. J Lumin 72–74:532–534
26. Xu QH, Fu LS, Li LS, Zhang HJ, Xu RR (2000) Preparation, characterization and photophysical properties of layered zirconium bis(monohydrogenphosphate) intercalated with rare earth complexes. J Mater Chem 10(11):2532–2536
27. Xu QH, Li LS, Liu XS, Xu RR (2002) Incorporation of rare-earth complex $Eu(TTA)_4C_5H_5NC_{16}H_{33}$ into surface-modified Si-MCM-41 and its photophysical properties. Chem Mater 14(2):549–555
28. Zhang MS, Yin W, Su Q, Zhang HJ (2002) Encapsulation and luminescence of the nanostructured supramolecular material [Eu $(Phen)_4](NO_3)_3/(CH_3)_3$Si-MCM-41. Mater Lett 57(4):940–945(6)
29. Fu LS, Zhang HJ, Wang SB, Meng QG, Yang KY, Ni JZ (1999) Preparation and luminescence properties of the ternary europium complex incorporated into an inorganic/polymer matrix by a sol–gel method. J Sol–Gel Sci Technol 15(1):49–55
30. Lenaerts P, Storms A, Mullens J, Haen JD, Görller-Walrand C, Binnemans K, Driesen K (2005) Thin films of highly luminescent lanthanide complexes covalently linked to an organic–inorganic hybrid material via 2-substituted imidazo[4,5-*f*]-1,10-phenanthroline groups. Chem Mater 17(20):5194–5201
31. Bekiari V, Pistolis G, Lianos P (1999) Intensely luminescent materials obtained by combining lanthanide ions, 2,2″-bipyridine, and poly(ethylene glycol) in various fluid or solid environments. Chem Mater 11(11):3189–3195
32. Bekiari V, Lianos P (2003) Photophysical studies on terpyridine-Eu^{3+} complexes in sol–gel nanocomposite materials. J Sol–Gel Sci Technol 26(1–3):887–890
33. Ji XL, Li B, Jiang SC, Dong DW, Zhang HJ, Jing XB, Jiang BZ (2000) Luminescent properties of organic–inorganic hybrid monoliths containing rare-earth complexes. J Non-Cryst Solids 275(1–2):52–58
34. Nakajima H, Kawano K (2006) Preparation and evaluation of the rare earth doped nanoparticle SiO_2–PVP hybrid thin film by sol–gel method. J Alloy Compd 408–412:701–705
35. Nakagawa K, Amita K, Mizuno H, Inoue Y, Hakushi T (1987) Preparation of some lanthanoid picrates and the behavior of their water of hydration. Bull Chem Soc Jpn 60(6):2037–2040
36. Parimala S, Gita KN, Kandaswamy M (1998) Synthesis, characterization, electrochemical studies and catecholase activity of a new series of binuclear copper(II) complexes. Polyhedron 17 (19):3445–3453
37. Bruker AXS (1998) SAINT software reference manual. Bruker AXS, Madison, WI
38. GM (1997) SHELXS-97 and SHELXL-97. Program for X-ray crystal structure solution and refinement. Gottingen University, Germany
39. Yang L, Yang R (1996) Synthesis and structure of didysprosium complexes with a tetraketone. J Mol Struct 380(1–2):75–84
40. Yu JB, Zhou L, Zhang HJ, Zheng YX, Li HR, Deng RP, Peng ZP, Li ZF (2005) Efficient electroluminescence from new lanthanide (Eu^{3+}, Sm^{3+}) complexes. Inorg Chem 44(5):1611–1618
41. Lakowicz JR (1983) Principles of fluorescence spectroscopy. Plenum, New York
42. Avnir D, Kaufman VR, Reisfeld R (1985) Organic fluorescent dyes trapped in silica and silica–titania thin films by the sol-gel method. Photophysical, film and cage properties. J Non-Cryst Solids 74(2–3):395–406